

Three-dimensional finite element simulation and application of high-strength bolts

Liji Long ^{*1}, Yongsong Yan ², Xinlin Gao ³ and Haigui Kang ⁴

¹ Faculty of Infrastructure Engineering Dalian University of Technology, China

² College of materials science and engineering chongqing university, China

³ China Communications 2nd Navigational Bureau 2nd Engineering Co., Ltd, China

⁴ Southwestern Hydro Engineering Research Institute For Water Way,
National Engineering Technology Research Center for Inland Waterway Regulation, China

(Received April 03, 2015, Revised October 09, 2015, Accepted November 12, 2015)

Abstract. High-strength structural bolts have been utilized for beam-to-column connections in steel-framed structural buildings. Failure of these components may be caused by the bolt shank fracture or threads stripping-off, documented in the literature. Furthermore, these structural bolts are galvanized for corrosion resistance or quenched-and-tempered in the manufacturing process. This paper adopted the finite element simulation to demonstrate discrete mechanical performance for these bolts under tensile loading conditions, the coated and uncoated numerical model has been built up for two numerical integration methods: explicit and implicit. Experimental testing and numerical methods can fully approach the failure mechanism of these bolts and their ultimate load capacities. Comparison has also been conducted for two numerical integration methods, demonstrating that the explicit integration procedure is also suitable for solving quasi-static problems. Furthermore, by using precise bolt models in T-Stub, more accurately simulate the mechanical behavior of T-Stub, which will lay the foundation of the mechanical properties of steel bolted joints.

Keywords: high-strength bolts; connections; thread stripping; finite element simulation

1. Introduction

Bolted connections are widely used in steel structures as they enable prefabricated beams and columns to be erected quickly on site without the complication and expense of on-site welding. The robustness of connections is essential for the transfer of loads from beams to columns to avoid progressive collapse. The two main factors, which affect the mechanical properties of the steel bolt nodes at a high temperature, have been concluded from real fire cases and fire experiments: the reduction of the strength of the bolt that caused by temperature rise; the additional force generated by the expansion of the steel bolt nodes in fire. Tested on bolts conducted by Godley and Needham in 1983 compared High Strength friction Grip (HSFG) and 8.8 grade bolts in tension and shear (Godley and Needham 1983). The tensile experiment explained the two failure modes of these bolts: tensile fracture of the bolt shank and thread stripping. In 1995, Kirby carried out a series of bolts experiments at high temperature to study the strength reduction for 8.8 structural bolts (Kirby

*Corresponding author, Ph.D., E-mail: ranfield106@gmail.com

1995). The results certify that under tension or shear force, bolts suffer the most dramatic intensity decrease at 300°C-700°C, and bolt fracture and thread stripping lead to the eventual destruction; the degree of matching between the bolt and the nut is vital in avoiding thread stripping; the nut intensity will also influence the final failure mechanism of the bolt; when the maximum temperature exceeds the temper point, the residual hardness of the bolt will decrease as the fire temperature increases. In 2007, Hu (Hu *et al.* 2007) proposed that bolt coating will affect the final failure modes of the bolt. In 2011, Burgess found that: the microstructure of the bolts that suffered plastic failure is pearlite and bainite, rather than tempered martensitic.

The above references, which have explored the two modes of bolt being damaged under high temperature, hasn't provided a finite-element simulation of detailed three-dimensional (3D) model yet. A large number of experimental data and project cases reveal that high-strength bolts in the steel structure are more prone to suffer thread stripping damage, rather than bolt shank fracture. However, in the finite element simulation, bolts are simplified to no thread without considering the influence of thread stripping, which will affect the accuracy of the finite element simulation results. As a result, the author of this paper has established a 3D model with a threaded bolt, and found out two kinds of failure mode of 8.8 grade high-strength bolts at normal temperature, as well as their load- displacement curve. The results are well matched with the experimental data. On this basis, the mechanical properties of the bolt in T-Stub components have also been explored, which lays the foundation for further studies.

2. The basic parameters of high-strength bolts

2.1 Tolerance class

The external thread includes three levels: 4h, 6h and 6g; the internal thread includes three levels: 5H, 6H, and 7H. For the metric thread, the basic deviation of H and h is zero; of G is positive; and of e, f and g are negative. As shown in Fig. 1.

As a tolerance zone position, H is commonly used in internal threads, and usually it is not used for surface coating or with a very thin layer. g is always for the 6-9 μm thin coating. General details on tolerance classes for high-strength hexagonal bolts are determined in accordance with specification of BS 4190 (BSI 2001) and BS EN ISO 4014 (CEN 2001) for the proposed helical thread model. Thread profile details are available in the specification of BS 3643-1 (BSI 1981) and ISO 965-5 (ISO 1998), as collected in Table 1. 8.8 grade high-strength bolts and nuts with the tolerance level for 6 H/g are used in the experiment of this paper.

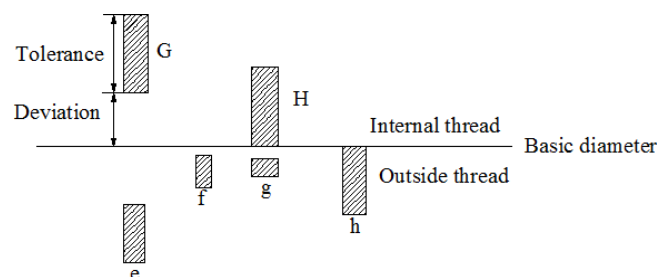


Fig. 1 Schematic of thread tolerance

Table 1 Dimension details of internal and external threads

Internal threads						External threads					
Tolerance class		Pitch	Major D	Pitch D2	Minor D1	Tolerance class	Pitch	Major D	Pitch D2	Minor D1	
6H	Min	2.5	20.000	18.376	17.294	6g	Min	2.5	19.623	18.164	/
	Max	2.5	20.224	18.600	17.744		Max	2.5	19.958	18.334	16.891
7H	Min	2.5	20.000	18.376	17.294	8g	Min	2.5	19.428	18.069	/
	Max	2.5	20.355	18.656	17.854		Max	2.5	19.958	18.334	16.891
6AX	Min	2.5	20.000	18.906	17.824	6az	Min	2.5	19.315	17.856	/
	Max	2.5	20.530	19.130	18.274		Max	2.5	19.650	18.026	16.583

Generally, to refrain from premature oxidation the surface of fasteners is coated, and 8.8 grade high-strength bolts are usually galvanized. This method, however, will exert negative effects on the mechanical property of bolts by reducing the effective area of the screw thread and leading to hydrogen embrittlement. The reasons for the generation of hydrogen embrittlement are complicated, and the degree of hydrogen embrittlement largely depends on the content of hydrogen that has invaded in the metal during its production or the process of galvanizing. In addition, the internal thread tapping of nuts should be 0.2-0.4mm to adapt to the additional coating. This process may lead to brittle failure (thread falling) (Hu and Zhao 2014) of bolts in the steel structure in the fire.

2.2 Material constitutive relations

In this investigation, the finite element software ABAQUS is used to establish an accurate three-dimensional spiral model connected with bolt tensile, and simulates the bolt stress distribution and failure pattern at room temperature (20°C). Considering the nonlinearity of the material, bilinear model is selected as the constitutive relation. The bilinear constitutive relation of the material at room temperature is obtained from the EC3 Part 1-2, and the constitutive relation of ordinary steel is listed. The specific data is as shown in Fig. 2.

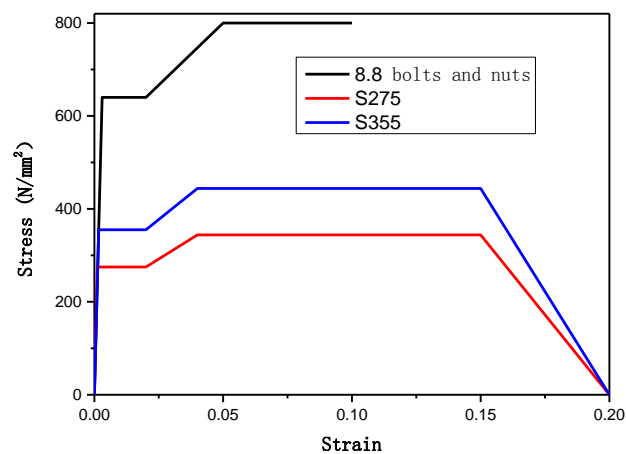


Fig. 2 Constitutive law of 8.8 high-strength steel bolts and structural steel

In order to accurately describe the plastic change of the material during the process of deformation, true stress and true strain must be used to define plastic material in ABAQUS. While most of the experimental data are nominal stress and nominal strain. At this point, the conversion formula is needed to change the plastic material data from the nominal stress/strain into true stress/strain (Yu *et al.* 2008). The formula is as follows

$$\sigma = \sigma_{nom} (1 + \varepsilon_{nom}) \quad (1)$$

$$\varepsilon = \ln(1 + \varepsilon_{nom}) \quad (2)$$

where: σ — true stress; ε — true strain;
 σ_{nom} — nominal stress; ε_{nom} — nominal strain

Table 2 Test grouping table

Bolt sets	Number	Bolt standards	Nut standards	Tolerance class
A	1,2,3	Grade 8.8 (BS 4190, Br)	Grade 10 (BS 4190, Br)	7H/8g
B	4,5,6	Grade 8.8 (ISO 4014, Br)	Grade 10 (ISO 4032, Br)	6H/6g
C	7,8,10	Grade 8.8 (BS 4190, Ba)	Grade 8 (BS4190, Ba)	7H/8g
D	9,11,12	Grade 8.8 (ISO 4014, Ba)	Grade 8 (ISO 4032, Ba)	6H/6g

* Br = Bright finish(zinc plated); Ba = Black finish.

Table 3 Test grouping table

Bolt sets	Number	Bolt failure	Failure stresses (N/mm ²)	Faliure load (kN)	Nut grade
A	Bolt 1	Bolt breakage	807.3	197.8	Grade 10
	Bolt 2		825.7	202.3	
	Bolt 3		728.6	178.5	
B	Bolt 4	Bolt breakage	978.4	239.7	Grade 10
	Bolt 5		956.7	234.4	
	Bolt 6		973.1	238.4	
C	Bolt 7	Threads stripping	780.0	191.1	Grade 8
	Bolt 8		745.7	182.7	
	Bolt 10		706.9	173.2	
D	Bolt 9	Threads stripping	750.2	183.8	Grade 8
	Bolt 11		806.5	197.6	
	Bolt 12		781.2	191.4	

3. The experiment survey

This article references 8.8 grade bolt tensile test in the reference (Hu *et al.* 2007), and bolts adopted in the experiment are from two different factories. The experiment was divided into four groups, which are shown in Table 2.

This experiment is segmented into two parts: under normal temperature and high temperature, while this paper only concerns the normal temperature. At the room temperature, the bolt components are installed in the universal testing machine to conduct the uniaxial tensile experiment until the specimen is damaged. During the experiment process, displacement is taken to control loading, and the control strain rate is 0.003 mm/min.

Table 3 summarizes the recorded failure load capacities for these bolt sets.

4. Finite Element Analysis (FEA)

4.1 Bolt Modeling and boundary conditions

The bolt connection system mainly includes bolts, nuts, gaskets and clamping piece. In order to reduce the computational cost, the gasket and the clamping piece are not considered in the model, while the load is uniformly distributed to act on the nut surface. This paper explores the bolt type ISO8765-M20×1.5×80×46, as shown in Fig. 3. A plated bolt model is established in consideration of the effect of bolt coating puts on the bolt failure mode, and the difference is that the nut thread overlap 0.4 mm. 3D models of the plated bolt possess 34796 units and 47327 nodes, while the 3D models of the uncoated bolt have 34715 units and 47183 nodes. Both of which the mesh types are



Fig. 3 Bolt appearance

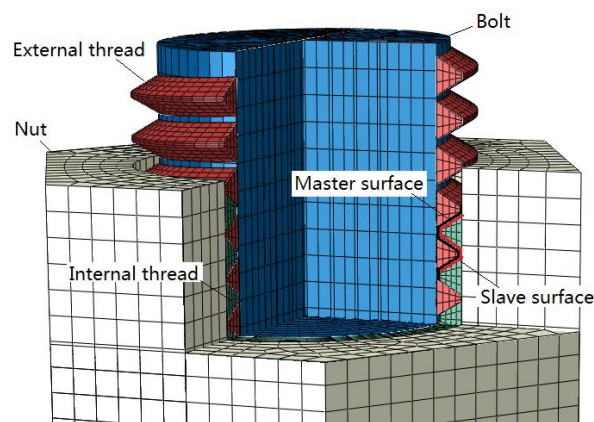


Fig. 4 Finite element mesh with boundary conditions

hexahedral meshes, and unit type with C3D8R. To facilitate the meshing, the bolt and thread modeling is separately conducted. The stress distribution of the thread is the most complicated when loaded (Ju *et al.* 2004), thus the meshing of the thread is more accurate, as shown in Fig. 4.

Regarding the FE model shown in Fig. 3, for the bolt cylinder, axial displacements are fully restrained at the bottom surface of a bolt, and the axial force is applied as a uniform displacement to a nut surface. For contact simulation, finite sliding is available for modeling the interaction between two contacting surfaces. Regarding contact friction, coefficients of friction μ are varied from 0.05 to 0.20, with coefficient of friction = 0.15 employed within this study. Master surfaces and slave surfaces are specified for internal and external threads, as illustrated in Fig. 4.

4.2 Selection of solver

Normally, stress that the bolt suffers changes much slow, and the bolt deformation is uniformly and sufficient, so the stress can be seen as the static function. In the process of the finite element simulation, ABAQUS/Standard, or ABAQUS/Explicit quasi static analysis can be taken to complete the stress process.

4.2.1 The comparison between explicit algorithm (ABAQUS/Explicit) and standard algorithm (ABAQUS/Standard)

(1) The Calculation Principle

Explicit algorithm is based on dynamic equation, so it is unnecessary for iteration. The central difference method of the structural dynamics is based on replacing displacement with the finite difference for the derivation of time. If take the same time step, such as $\Delta t(i) = \Delta t$ (Δt is a constant), with u as the displacement, then the equation of the center of speed and acceleration approximately to (Dai *et al.* 2010)

$$u'(i) = \frac{[u(i+1) - u(i-1)]}{2\Delta t} \quad (3)$$

$$u''(i) = \frac{[u(i+1) - 2u(i) + u(i-1)]}{(\Delta t \times \Delta t)} \quad (4)$$

Implicit algorithm is based on D'Alembert principle, and usually need an iterative calculation. In implicit algorithm, each incremental step needs an iterative calculation to solve static equilibrium equation, and each iteration needs to solve large linear equations, which may take up a considerable amount of computing resources, disk space and internal memory.

(2) Time Computation

In the explicit integration method, the calculation cost is proportional to the number of units, and is roughly inversely proportional to the size of the smallest unit. While in the implicit integration method, the calculation cost is roughly proportional to the square of the number of degrees of freedom (Barata *et al.* 2014).

4.2.2 Quasi-static simulation implementation

By controlling the loading speed, the dynamic explicit analysis can be used to simulate quasi-static. There are always two problems in the process of simulation: first, when the loading speed is too fast, the structure dynamic effect may occur; second, for static loading, the introduction of

inertial force may cause overestimation of the actual bearing capacity of the structure (Zhou and Feng 2009).

For the former, loading speed is related to the structural natural frequencies. In general, the load time of steel components should be 0.1-1s, and the more flexible it is, the longer the load time should be. For the latter, there are two kinds of methods: one is to inspect the ratio of kinetic energy and internal energy. As ABAQUS/Explicit puts it, for the quasi-static analysis, the ratio of kinetic energy and internal energy should be less than 10%, and results that are greater than 10% should be classified as having generated dynamic effect (Dang *et al.* 2013); second, when the structure is under static effect, counterforce should be roughly equal with force.

5. The finite element simulation results analysis

In this paper, the experiment has carried on the finite element simulation with group A (bolts 1, 2, 3) and group D (bolts 9, 11, 12), and Figs. 5 and 6 show the contrast between the two failure modes.

Both the experiment and the finite element simulation results show that the coating bolt screw thread stripping damage happened, while the uncoated bolt necking damage happened. In order to avoid dynamic effect of the ABAQUS/Explicit calculation result, the ratio (Zhuang *et al.* 2005) of its kinetic energy and internal energy should be verified, as shown in Fig. 7.

During the previous 0.1 seconds, the ratio of kinetic energy and internal energy is over 10%, which are due to the sudden speed change of the components when loading, leading to a big internal energy ratio. When the loading enters into a smooth phase, the dynamic effect of the bolt



Fig. 5 Failure mode of galvanized bolts



Fig. 6 Failure mode of normal bolts

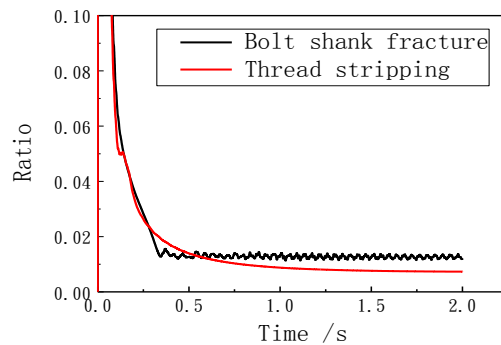


Fig. 7 The specific values between kinetic energy and internal energy

Table 4 Ultimate capacity of bolt

Bolt sets	Ultimate capacity (KN)	Test (mean)	Explicit		Standard	
			Result	Deviation	Result	Deviation
A		192.8	193	0.10%	180	6.64%
D		190.9	195.5	2.41%	181.9	4.71%

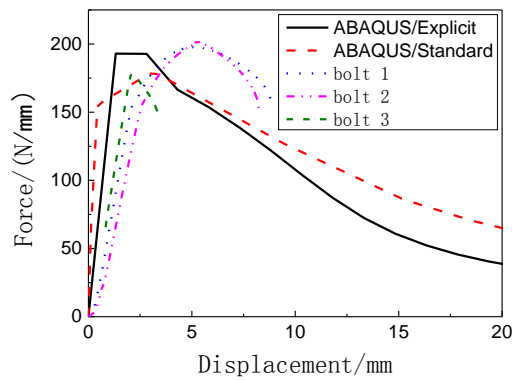


Fig. 8 Load-displacement curve of normal bolts

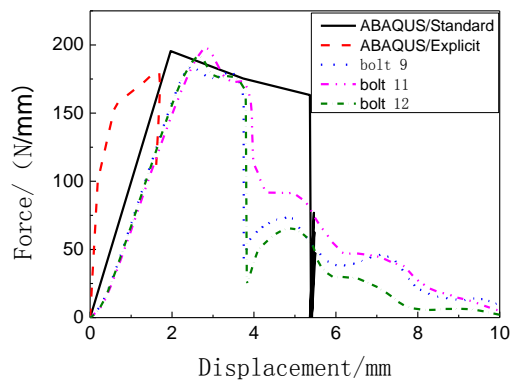


Fig. 9 Load-displacement curve of galvanized bolts

components is significantly reduced and the ratio of internal energy and kinetic energy is less than 10%, it can be seen as static load (Lu *et al.* 2011).

By using ABAQUS/Standard and ABAQUS/Explicit, the ultimate bearing capacity and the load-displacement curve of the bolt tensile are obtained, as shown in Table 4 and Figs. 8 and 9.

Due to different production processes of bolt sets B, its failure stresses is higher than normal bolts. In view of this, the test results of two bolt sets A and D, which represent two different failure modes, were employed to verify the numerical models. The results demonstrate that the maximum bearing capacity of the bolt obtained by using ABAQUS finite element software is close to the test result, and the results of the dynamic explicit algorithm are more consistent with the test.

In the load-displacement curve, compared with the experimental results, the bigger of the initial slope of the curve in the finite element simulation largely attributes to two aspects. One is the small gap (Yu *et al.* 2008) between the bolt and nut interface cannot be eliminated when using the displacement meter to measure longitudinal compression ratio; the other is the actual specimen has residual stresses, which reduces the cross-section stiffness (Hanus *et al.* 2011).

6. The Application of the 3D Accurate High-strength Bolt Model in T-Stub

In the semi-rigid connections, T-Stub is a common assembly. Following is a case from the reference (Abidelah *et al.* 2014), which aims to explore the mechanical property of the detailed and simplified bolt model in T-Stub.

6.1 The detailed dimensions and material property of T-stub assembly

Under tension, T-Stub assembly can be converted to two failure modes, including the plastic yielding of end-plate and the damage of high-strength bolt. This investigation focus on exploring the possible effect that the detailed and simplified bolt model might bring to the mechanical property of T-Stub. Therefore, according to the reference (Abidelah *et al.* 2014), it is assumed that

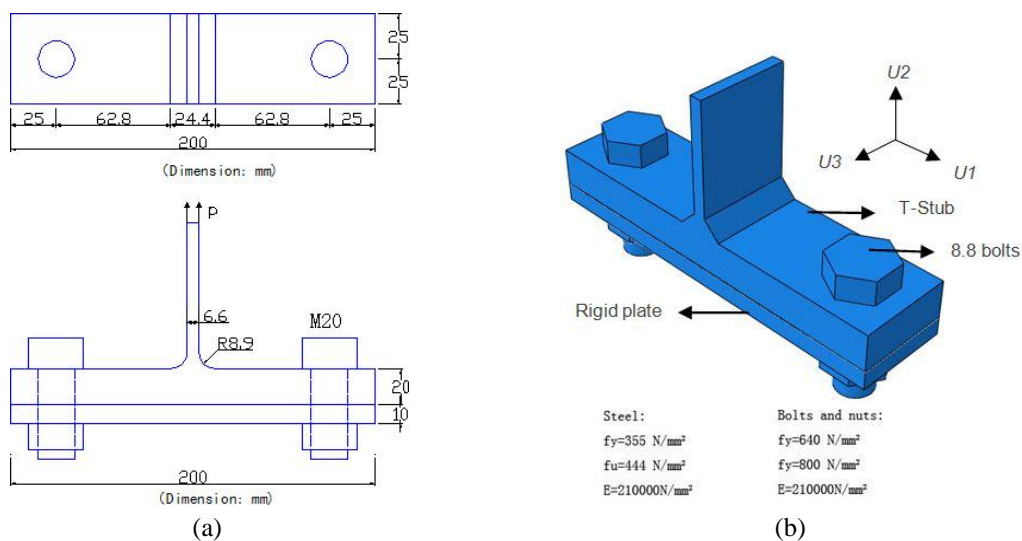


Fig. 10 T-Stub component dimensions and material parameters in detail

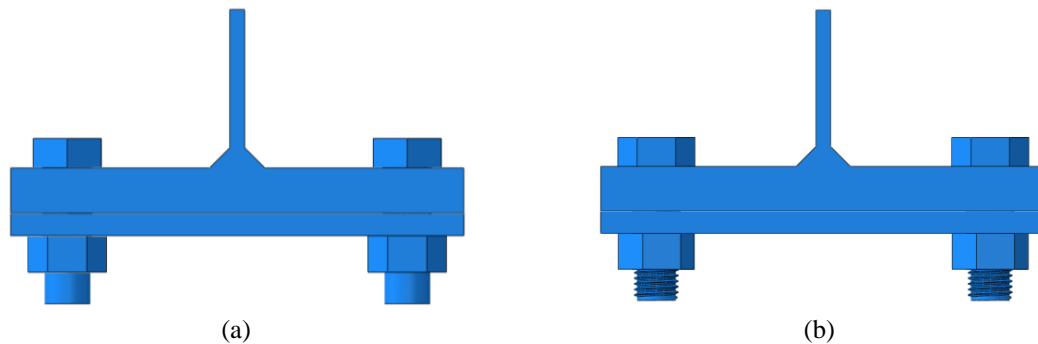


Fig. 11 Simplified and accurate finite element model of T-Stub component

plate thickness is $t_p = 20$ mm and web thickness is $t_w = 6.6$ mm, galvanized bolts which are same with group D are employed. The detailed dimensions of T-Stub assembly are as shown in Fig. 10. For contact simulation, finite sliding is available for modeling the interaction between two contacting surfaces. The coefficient of friction is also 0.15 in this study.

6.2 The two finite element models and their result comparison

The two models both have adopted the implicit dynamic calculations, and have taken the 3D brick element as the element type. With the consideration of the possible slip on the bolts, a kind of threaded bolt model is established in the detailed finite element model. While it is supposed that there is no slip in the simplified finite element model, that is, necking damage on bolt, which means it is not necessary to build the threaded bolt in this kind of model. The two models are as shown in Fig. 11.

With the purpose of gaining a better astringency, the displacement control loading should be applied in the whole loading procedure. The rigid plate is assumed to be $u_1 = 0$, $u_2 = 0$ and $u_3 = 0$. The coupling function of the ABAQUS can autonomously figure out the horizontal reaction. The force-displacement diagram of the web plate is illustrated in Fig. 12.

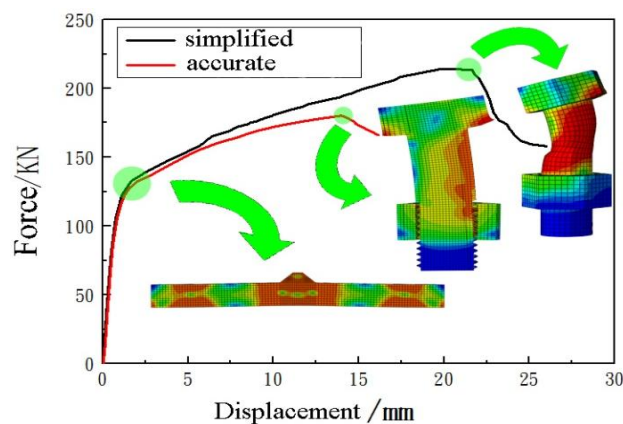


Fig. 12 Comparison of two finite element models calculated results

According to the result comparison of the two models, there is almost no difference between them. However, with the slip of bolt in the detailed model, its carrying capacity reaches its maximum 175 KN. On the contrary, the ultimate carrying capacity can reach 221 KN in the simplified model until necking has happened in its bolt.

It is obvious to find that the first inflection point of the force-displacement curves of the accurate and simplified finite element models are very close, which is arisen from the plastic yield of bolt holes and the web flange. And after that, resistance to T-Stub components is mainly provided by the bolt. As the load continues, the threaded bolt of the accurate model yields and slips, and the bearing capacity reaches its maximum and begin to unload; while the simplified model reaches its ultimate bearing capacity after the bolt necking.

7. Conclusions

The finite element analysis software ABAQUS is employed in this article to simulate the coating and uncoated 3D accurate bolt models, which has further confirmed that coating bolt, is prone to suffer thread stripping damage.

- (1) Comparing the finite element simulation results with the experiment results, it can be discovered that for the ultimate bearing capacity, standard and implicit algorithm are both in a good agreement with the experiment; for the load - displacement curve, standard algorithm is more approach to the experiment results.
- (2) ABAQUS/Explicit analysis module is equipped with specific usages, which is not just applied to simulate short, instantaneous dynamic events, but also to tackle with complex contact condition and highly nonlinear quasi-static problem.
- (3) In the steel structure finite element simulation, the majority bolts in connections are simplified as no thread model which will save time cost, however, the calculation accuracy will be affected to a certain extent. As a consequence, threaded bolt might be adopted in the simulation of steel structure.
- (4) In T-Stub, the bearing capacity is similar between the accurate model and the simplified model, while the accurate model is more truthful in reflecting the real stress distribution in the T-Stub. Bolt thread stripping failure is highly common, which is often neglected in the finite element simulation. This paper further confirmed that the accurate bolt model can be implemented in the finite element simulation, which will be instrumental to study the mechanical properties of the steel structure bolts node by using numerical simulation method.

References

- Abidelah, A., Boucha, A.R. and Kerdal, D.E. (2014), "Influence of the flexural rigidity of the bolt on the behavior of the T-stub steel connection", *Eng. Struct.*, **81**, 181-194.
- Barata, P., Riberio, J., Rigueiro, C., Santiago, A. and Rodrigues, J. (2014), "Assessment of the T-stub joint component at ambient and elevated temperatures", *Fire Safe. J.*, **70**, 1-13.
- BSI (1981), BS 3643-1: 1981 ISO Metric Screw Threads – Part 1: Principles And Basic Data ISO, British Standard Institution, London, UK.
- BSI (2001), BS 3692:2001 ISO metric precision hexagon bolts, screws and nuts – Specification, British Standards Institution, London, UK.
- CEN (2001), BS EN ISO 4014: 2001 Hexagon head bolts – Products grades A and B, European Committee

- for Standardisation, Brussels, Belgium.
- Dai, X.H., Wang, Y.C. and Bailey, C.G. (2010), "Numerical modeling of structural fire behavior of restrained steel beam-column assemblies using typical joint types", *Eng. Struct.*, **32**(8), 2337-2351.
- Dang Hoang, T., Herbelot, C., Imad, A. and Benseddiq, N. (2013), "Numerical modelling for prediction of ductile fracture of bolted structure under tension shear loading", *Finite Elem. Anal. Des.*, **67**, 56-65.
- Godley, M.H.R. and Needham, F.H. (1983), "Comparative tests on 8.8 and HSFG bolts in tension and shear", *Struct. Engr.*, **60**(3), 21-26.
- Hanus, F., Zilli, G. and Franssen, J.M. (2011), "Behavior of Grade 8.8 bolts under natural fire conditions—Tests and model", *J. Construct. Steel Res.*, **67**(8), 1292-1298.
- Hu, Y. and Zhao, P.F. (2014), "A review on fire resistance of high-strength bolts", *Proceedings of the 23th National Conference on Structural Engineering*, Lanzhou, China, October, pp. 223-227. [In Chinese]
- Hu, Y., Davison, J.B., Burgess, I.W. and Plank, R.J. (2007), "Comparative study of the behavior of BS 4190 and BS EB ISO 4914 bolts in fire", *Proceedings of the 3rd International Conference on Steel and Composite Structures*, Manchester, UK, July-August, pp. 587-592.
- ISO 965-5 (1998), ISO general purpose metric screw threads – tolerances – Part5: Limits of sizes for internal screw threads to mate with hot-dip galvanized external screw threads with maximum size of tolerance position h before galvanizing, British Standard Institution, London, UK.
- Ju, S.H., Fan, C.Y. and Wu, G.H. (2004), "Three-dimensional finite elements of steel bolted connections", *Eng. Struct.*, **26**(3), 403-413.
- Kirby, B.R. (1995), "The behavior of high-strength grade 8.8 bolts in fire", *J. Construct. Steel Res.*, **33**(1-2), 3-38.
- Lu, W., Pentti M., Jyri, O. and Ma, Z.C. (2011), "Design of screwed steel sheeting connection at ambient and elevated temperatures", *Thin-Wall. Struct.*, **49**(12), 1526-1533.
- Yu, H., Burgess, I.W., Davison, J.B. and Plank, R.J. (2008), "Numerical simulation of bolted steel connections in fire using explicit dynamic analysis", *J. Construct. Steel Res.*, **64**(5), 515-525.
- Zhou, H.T. and Feng, Z.H. (2009), "Research on ultimate bearing capacity of high-strength bolted connections", *J. Wuhan Univ. Technol.*, **2009**(9), 49-51. [In Chinese]
- Zhuang, Z., Zhang, F. and Cen, S. (2005), "ABAQUS nonlinear finite element analysis and examples", *Science Press*, 314-321. [In Chinese]